micro

MDPI

Article

Assessment of Pharmaco-Technological Parameters of Solid Lipid Nanoparticles as Carriers for Sinapic Acid

Stefano Russo, Giuliana Greco and Maria Grazia Sarpietro *

Department of Drug and Health Sciences, University of Catania, Viale Andrea Doria 6, 95125 Catania, Italy
* Correspondence: mg.sarpietro@unict.it

Abstract: Sinapic acid, 3,5-dimethoxyl-4-hydroxycinnamic acid, belonging to the class of hydroxycinnamic acids, shows antioxidant, anti-inflammatory, anticancer, hepatoprotective, cardioprotective, renoprotective, neuroprotective, antidiabetic, anxiolytic, and antibacterial activity. The aim of this work was to incorporate sinapic acid into solid lipid nanoparticles in order to improve its bioavailability. SLNs were prepared using the hot high-speed homogenization method. The pharmaco-technological properties and thermotropic profile of SLNs encapsulated with sinapic acid, as well as their interaction with biomembrane models, were evaluated. SLNs showed promising physico-chemical properties and encapsulation efficiency, as well as a desirable release profile; moreover, they facilitated the interaction of sinapic acid with a biomembrane model made of multilamellar vesicles. In conclusion, this formulation can be used in further studies to assess its suitability to improve sinapic acid activity.

Keywords: sinapic acid; SLN; biomembrane model

check for updates

Citation: Russo, S.; Greco, G.; Sarpietro, M.G. Assessment of Pharmaco-Technological Parameters of Solid Lipid Nanoparticles as Carriers for Sinapic Acid. *Micro* **2023**, *3*, 510–520. https://doi.org/10.3390/micro3020034

Academic Editor: Horacio Bach

Received: 23 March 2023
Revised: 27 April 2023
Accepted: 2 May 2023
Published: 5 May 2023

1. Introduction

Sinapic acid, 3,5-dimethoxyl-4-hydroxycinnamic acid (Figure 1), belongs to the class of hydroxycinnamic acids (specifically, the subclass of phenolic acids. These compounds have radical-scavenging activity, represented by the ability to donate an electron to neutralize free radicals (reported to be responsible for oxidative stress) [1]. Among other hydroxycinnamic acids, according to in vitro noncellular studies (DPPH assay), caffeic acid and ferulic acid exhibit similar properties to sinapic acid [2].

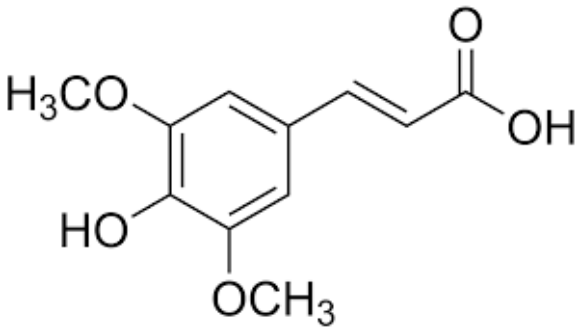

Figure 1. Chemical structure of sinapic acid.

Sinapic acid is abundantly found in different plant species, e.g., strawberries and cranberries, as well as cereals and vegetables; it is one of the most common compounds in the Brassicaceae family. Data found in the literature show that sinapic acid possesses antioxidant and anti-inflammatory properties [3], as well as anticancer [4], hepatoprotective [5], cardioprotective [6], renoprotective [6], neuroprotective [7], antidiabetic [8], anxiolytic [9], and antibacterial activity [10]. A review of the pharmacological and therapeutic applications

of sinapic acid was recently published by Pandi et al. [11]. Sinapic acid exists in nature in free form, in ester form, or conjugated with a sugar (glycoside). Some esterified derivatives of sinapic acid such as sinapine, 4-vinylsyringol, and syringaldehyde have also exhibited acetylcholinesterase-inhibitory, antimutagenic, and antioxidant activity, respectively [11]. In [12], it was observed that esterification of sinapic acid decreased its bioavailability [13] and made it a substrate of esterase enzymes, located in the small intestine and colon; its hydrolysis yields the free form that is subsequently adsorbed. Although esters of sinapic acid possess lower antioxidant activity than the free molecule, the lipophilicity of these compounds is increased, ensuring a greater affinity for the lipophilic phase of certain drug delivery systems and, most importantly, the cell membrane [14].

Solubility can be a parameter that influences drug bioavailability [15]. Phenolic acids are often poorly soluble [16], and it has been reported that sinapic acid is the least soluble among hydroxycinnamic acids (caffeic, ferulic, o-coumaric, m-coumaric, and p-coumaric acids) [17]. Accordingly, it is possible that poor solubility and, thus, low bioavailability could limit the potential therapeutic effect of sinapic acid. With this in mind, studies have been conducted to improve the solubility of sinapic acid. Cocrystals of sinapic acid with nicotinamide were obtained in [18]. The inclusion of sinapic acid in hydroxypropyl-cyclodextrin improved its solubility [19]. Many phenolic compounds are poorly absorbed and are metabolized into inactive forms, resulting in low blood concentrations [20]. Thus, the encapsulation of sinapic acid in solid lipid nanoparticles (SLNs) could solve problems related to its low solubility and rapid metabolism, thus achieving a better therapeutic potential as a function of a slow, protected release of the molecule on cellular substrates. In this study, sinapic acid was encapsulated in SLNs, colloidal carrier systems that find use not only in the pharmaceutical, but also in the cosmetic field [21]. SLNs are produced using lipids which are in a solid state at room and body temperature, as well as various surfactants. SLNs offer different interesting properties such as a small size (50–1000 nm) and huge surface area [22]. Compared to other drug delivery systems, SLNs possess advantages such as excellent biocompatibility, thanks to the employment of GRAS lipids, modulation of drug release over time, drug targeting, and protection of active compounds from degradation reactions [23,24]. Natural active compounds have been successfully encapsulated in SLNs [25,26]. Several techniques have been developed for the production of SLNs, e.g., high-pressure homogenization (HPH) by Muller et al. and the microemulsion technique by Gasco. The aim of this work was to evaluate the pharmaco-technological properties and thermotropic profile of SLNs encapsulating sinapic acid, as well as their interaction with biomembrane models. These results could be useful for subsequent studies related to the prevention and treatment of many disorders whose development is associated with oxidative stress.

2. Materials and Methods

2.1. Materials

Cetyl palmitate was obtained from A.C.E.F S.p.a (Piacenza, Italy). Sinapic acid (SA, purity up to 98%) and Tween®-80 were obtained from Sigma-Aldrich (Milan, Italy). Dimyristoylphosphatidylcholine (DMPC) was purchased from Genzyme (Liestal, Switzerland).

2.2. Preparation of SLNs

SLNs were formulated using the hot high-speed homogenization (HSH) method [27]. The lipid phase containing cetyl palmitate (166.8 mg) was warmed at 80 °C; the same temperature was used to heat the aqueous phase consisting of water (up to 20 mL) and Tween-80 (66.8 mg), whereby the latter was slowly added to the lipid phase under agitation. The obtained emulsion was subjected to homogenization using a high-pressure homogenizer (UltraTURRAX-IKA-T18-basic, IKA-Werke, Staufen, Germany) at 12,300 rpm for 10 min at 80 °C. SLNs were prepared as empty (SLN) or loaded with 10% *w*/*w* sinapic acid (SLN-SA) with respect to cetyl palmitate.

2.3. Characterization of SLNs

The particle size, polydispersity index (PDI), and zeta potential (ZP) of the nanoparticles were determined at room temperature through dynamic light scattering (DLS) and electrophoretic light scattering using a Zeta Sizer Nano-ZS90 (Malvern Instrument Ltd., Worcs, UK), equipped with a laser with a nominal power of 4.5 mW and a maximum power of 5 mW at 670 nm. The analyses were performed using a 90° scattering angle at 20 ± 0.2 °C. The analyses were carried out for 2 months. The morphologies were investigated using field-emission scanning electron microscopy (FE-SEM; ZEISS SUPRA 55 VP; White Plains, NY, USA). All FE-SEM images were recorded at an operating voltage of 10 kV with a working distance of 5.5 mm, using the in-lens secondary electron detector.

2.4. Encapsulation Efficiency

Two different methods were used to calculate the encapsulation efficiency.

Method 1.

A dialysis membrane (Spectra/Por Dialysis Membrane MWCO: 2.000, wet in 0.1% sodium azide) containing 2 mL of pure water was placed inside an exact amount of sinapic acid-loaded SLNs (SLN-SA) at 25 °C under stirring for 24 h. The amount of sinapic acid that diffused through the membrane was determined spectrophotometrically (UV/Vis Lambda 25, PerkinElmer, Frankfurt/Main, Germany) using a previously made calibration line. The amount of sinapic acid encapsulated in the SLN was calculated as the difference between the total amount of sinapic acid in the preparation and in the solvent [28].

Method 2.

The entrapment efficiency was determined by measuring the concentration of free drug in aqueous medium as reported previously [29]. The aqueous medium was separated using Vivaspin 2 Centrifugal Concentrators (Sartorius, UK) possessing a filter membrane (MWCO 2000 Da). An exact amount of SLN-SA (whole formulation) was placed inside the test tube and submitted to centrifugation at 5000 rpm for 30 min (Centrifuge 5804/5804 R Beckman; A-4-44). The amount of SA in the aqueous phase was determined using a spectrophotometer (UV/Vis Lambda 25, PerkinElmer). The amount of sinapic acid encapsulated in the SLN was determined by the difference between the total amount of sinapic acid used and that present in the solvent [30].

2.5. In Vitro Drug Release

The in vitro drug release was studied using the dialysis tube method [31]. Briefly, 1 mL of SLN-SA (whole formulation) [32] was placed inside a dialysis tube (Spectra/Por Dialysis Membrane MWCO: 2.000, wet in 0.1% sodium azide). The latter was put into a glass beaker containing water at 25 °C under stirring. At predetermined intervals (from 30 min to 10 h), a 1 mL aliquot was withdrawn from the beaker and replaced with fresh media. The amount of sinapic acid was determined spectrophotometrically.

2.6. Preparation of MLV

MLV were prepared both in absence and in presence of Sinapic Acid. The first were used as biological membrane models to evaluate their interaction with Sinapic Acid loaded-SLN, while the second were prepared to evaluate the effect of the compound on the MLV's thermotropic behavior. Solutions of 1,2-Dimyristoyl-Glycerol-3-phosphatidylcholine (DMPC) and Sinapic Acid in chloroform/methanol (1:1, *v*:*v*) were prepared. Aliquots of the DMPC solution as to have 7 mg of DMPC in each tube were delivered in glass tubes. Aliquot of the Sinapic Acid solution was added to the glass tubes as to have the same stoichiometric ratio of Sinapic Acid contained in the SLN to study the interaction between the biomembrane model and SLN. The solvents were evaporated under nitrogen flow (in a water bath at 37 °C) to obtain lipid films. Then, the samples were subjected to freeze-drying for 3 h to remove any solvent residues. 168 µL of 50 mM TRIS solution (pH = 7.4), was added. The samples were heated in a water bath at 37 °C for 1 min and vortexed for 1 min (the procedure was repeated three times) and then kept at 37 °C for 1 h [33].

2.7. DSC Analysis

Calorimetric analysis was performed using a Mettler Toledo STAR^e system (Switzerland) equipped with a DSC1 calorimetric cell. Mettler TA-STAR^e software (version 16.00) was used to obtain and analyze data. The sensitivity was automatically chosen as the maximum possible by the calorimetric system. The calorimeter was calibrated using Indium (99.95% of purity), based on the setting of the instrument. 160 µL aluminum calorimetric pans were used. The reference pan was filled with 120 µL of deionized water.

2.7.1. Calorimetric Analysis of SLNs and MLVs

Aliquots of 120 µL of the samples were transferred into 160 µL DSC aluminum pans hermetically sealed and subjected to calorimetric analysis under Nitrogen flow (60 mL/min) as follows:

- Heating from 5 °C to 70 °C, at 2 °C/min.
- Cooling from 70 °C to 5 °C, at 4 °C/min.

The samples were cooled and heated three times to check the reproducibility of results.

2.7.2. SLN/MLV Interaction

First, 60 µL of MLVs and 60 µL of SLNs (loaded with SA 10% *w*/*w*) were placed into a 160 µL crucible which was hermetically sealed and subjected to calorimetric analysis as follows: a heating scan from 5 to 70 °C (heating rate 2 °C/min), a cooling scan from 70 to 37 °C (cooling rate 4 °C/min), an isothermal period (1 h) at 37 °C, and a cooling scan from 37 to 5 °C (cooling rate 4°C/min). This procedure was repeated seven times to evaluate the interaction between SLNs and MLVs over time.

2.8. Statistical Analysis

Statistical analysis was performed using GraphPad Prism 9.0.0 software (Boston, MA, USA); the algorithm employed was ordinary two-way ANOVA with multiple group comparisons corrected by the Sìdak test.

3. Results

3.1. SLN Characterization

SLNs (empty or loaded with SA) had particle sizes around 200 nm, with a mild growth trend over time. PDI values were around 0.300, suggesting the presence of a rather homogeneous population of nanoparticles in the investigated samples. ZP proved to be on the order of the −30 mV, indicating an optimal electric potential that prevents particle aggregation. The measurements remained almost unchanged in the chosen time period (up to 2 months), indicating that the formulations were stable (Figure 2). No significant difference between SLN and SLN-SA was noted from the statistical analysis, although SLN-SA was demonstrated to be slightly bigger, hinting at the fact that 10% *w*/*w* SA was insufficient to alter the pharmaco-technological parameters of SLN.

SEM analyses (Figure S1, Supplementary Materials) confirmed the PCS data, underlining the correct dimensions and the overall good morphologies of the formulated samples.

3.2. Entrapment Efficiency

The entrapment efficiencies of SLN-SA were obtained using two different methods (described in Section 2.4). The entrapment efficiencies obtained were quite comparable; in fact, using Method 1, an entrapment efficiency of 74.4% was obtained, whereas, using Method 2, an entrapment efficiency of 73.5% was obtained. The formulation permits encapsulating an important fraction of SA.

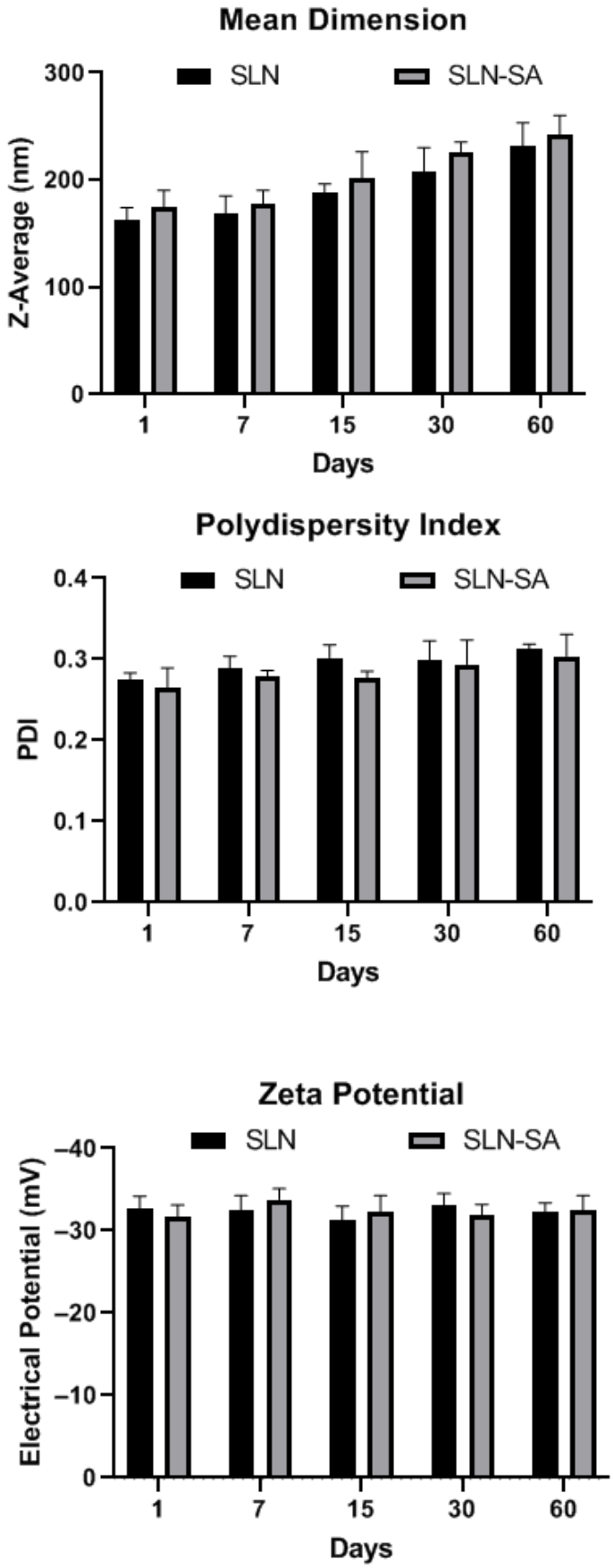

Figure 2. Mean dimensions, PDI, and ZP of SLNs and SLN-SA over 2 months.

3.3. In Vitro Release Study

The dialysis bag method described in Section 2.5 was used to evaluate the release of sinapic acid from SLN-SA. The percentage of sinapic acid released in water is shown in Figure 1. After 30 min, 26% of the total sinapic acid was released, reaching a theoretical plateau of 33.5% after 150 min. A slow release was noted up to 650 min (Figure 3). These data could be fitted to a hyperbolic curve, with a burst release at 30 min, and a slow, long-lasting release after this timepoint, attributed to the liberation of encapsulated sinapic acid from SLNs.

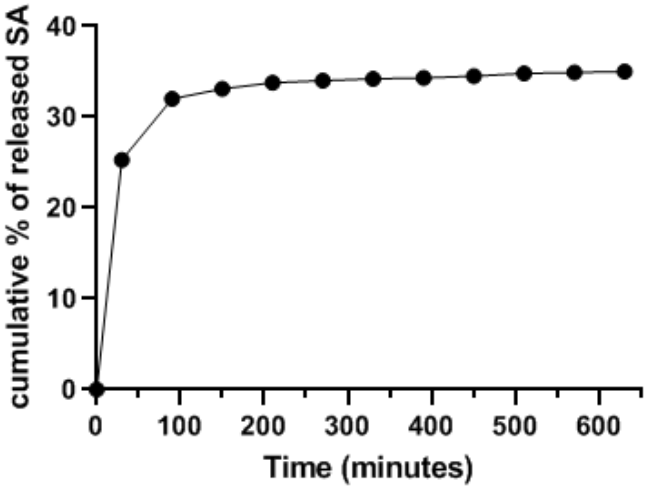

Figure 3. In vitro release profile of sinapic acid.

3.4. DSC Analysis

3.4.1. SLN Calorimetric Analysis

The curves of SLNs and SLN-SA are shown in Figure 4. The curve of unloaded SLNs showed a main peak at 55 °C and a broad shoulder below the main transition point. The thermotropic behavior of SLN-SA was similar to that of unloaded SLNs (slightly higher T_m, no shoulder), with little but distinct variations in temperature and shape. These results could be attributed to the formation of clusters of sinapic acid within the SLN structure, with moderate influences on the thermotropic behavior and crystallinity of the lipid components.

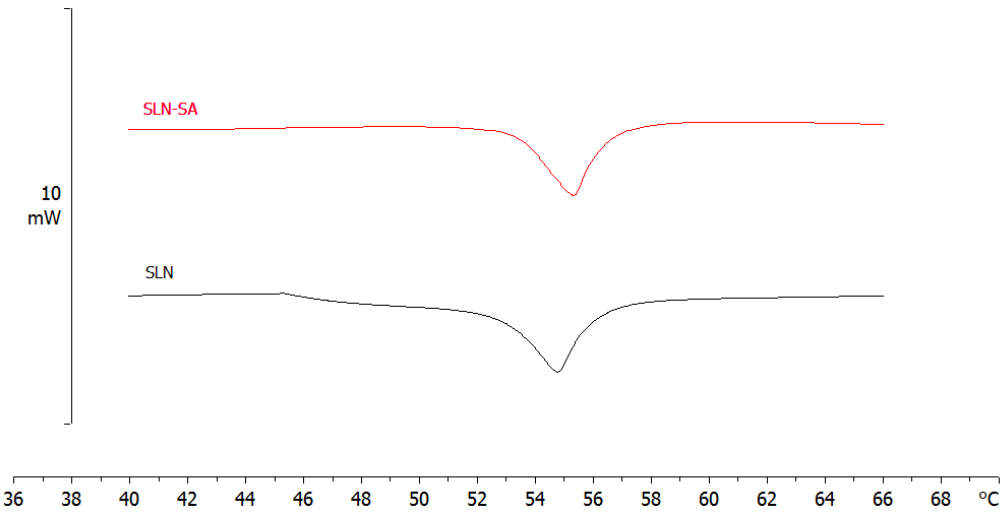

Figure 4. DSC thermograms of SLN vs. SLN-SA.

3.4.2. Calorimetric Analysis of MLVs

In the MLV calorimetric thermogram, two peaks associated with phase transitions were present: the pre-transition peak, at about 17 °C, due to the transition from the gel ordered phase to the ripple phase; the main transition peak, at about 25 °C, caused by the transition from the ripple phase to the gel liquid crystalline disordered phase [34]. In the MLVs prepared with SA at the same stoichiometric ratio as SLN-SA, significant variations were present; while the main transition temperature did not change much (0.5 °C lower), enthalpic energy decreased by around 23%, and the pre-transition peak disappeared entirely (Figure 5). It has been proposed that the pre-transition is due to the rotation of the polar headgroups of the phospholipid molecules [35], with head group hydration also playing an important role in rippled phase formation [36]. Then, the pre-transition is affected by the presence of foreign molecules on the bilayer surface [37]. The suppression of the pre-transition suggests a direct interaction of sinapic acid with the DMPC head group [38]. In the presence of sinapic acid, a unique main transition peak of MLV was present. The presence of a unique peak or the appearance of shoulders allows obtaining information on the distribution of a molecule in the MLV; the shoulders are attributed to a nonideal mixing behavior, which creates a nonhomogeneous distribution of the molecule within the membrane, whereas the absence of shoulders hints at a uniform distribution of SA inside the MLV [39,40]. Taken together, these results prove that sinapic acid did affect the acyl chain packing of the bilayer, suggesting (given the logP of SA = 1.6) a localization between the aqueous and lipid compartments of MLV [41].

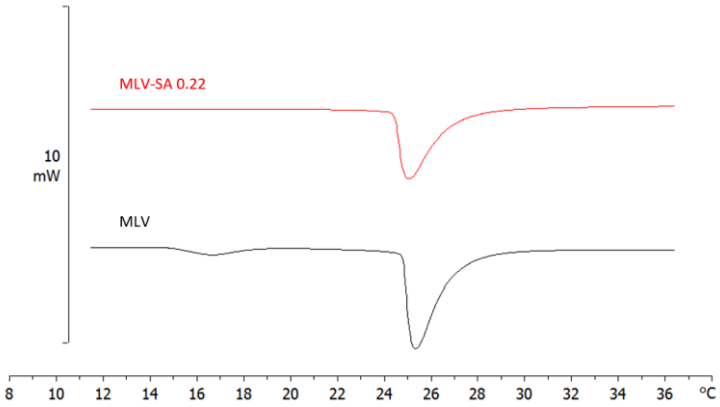

Figure 5. DSC thermograms of MLV vs. MLV-SA.

3.4.3. SLN/MLV Interaction

An experiment was carried out to evaluate the ability of SLN to act as carrier for sinapic acid and allow cell penetration; for this reason, the interaction of SLN-SA with MLVs was studied, with the latter being used as a biomembrane model [42]. MLVs and SLN-SA came into contact following the methodology described in Section 2.7.2, and the samples were analyzed immediately and at regular intervals after being mixed. The interaction between SLN-SA and MLVs was assessed through the changes in their thermograms (Figure 6). MLVs lost the pre-transition peak upon contact with SLNs; the main transition peak shifted to slightly lower temperatures and, as time increased, its enthalpy decreased until reaching, at the last scan, a value similar to that achieved when preparing MLVs with 0.22 of sinapic acid. The presence of a unique peak all along the measurements could indicate a uniform distribution of sinapic acid in the MLV structure. The calorimetric peak related to SLNs moved to lower temperatures, and its enthalpy decreased over time. Therefore, SLN interactions with biomembranes could account for their ability to allow sinapic acid penetration into the cell membrane, permitting its uptake by the cells while protecting it from metabolic reactions.

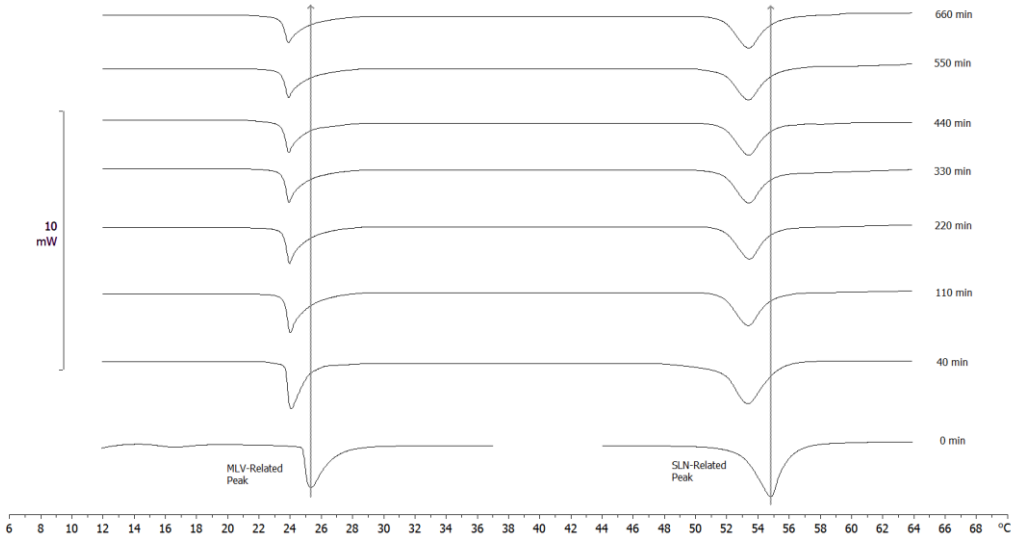

Figure 6. Calorimetric curves, in heating mode, of MLVs and SLN-SA put in contact and mixed, at increasing times of incubation. Curves at 0 min refer to MLVs and SLN-SA before the contact. The time of contact is reported on the right side of the curves.

4. Discussion

Sinapic acid exhibits similar pharmacological proprieties to active compounds within the same class of hydroxycinnamic acids, such as ferulic or caffeic acid. Sinapic acid has been demonstrated to play an important biomedical role, as underlined by the great number of experiments performed both in vitro and in rats and mice [9]; these studies highlighted the anxiolytic-like effects of sinapic acid due to its interaction with $GABA_A$ receptors. Other studies revealed the effect of SA on glucose metabolism, whereby it reduced the hyperglycemia of diabetic rats and attenuated the postprandial plasma glucose without changing plasma insulin in rats [43]. It was reported that sinapic acid has remarkable antioxidant properties and could alleviate oxidative stress and intestinal dysbiosis induced in rats [44].

However, the drawback of sinapic acid is its rapid metabolization and excretion in a free and glucoronate form; thus, a way to improve these pharmacokinetic properties is its encapsulation in solid lipid nanoparticles.

The aim of this study was to encapsulate sinapic acid into SLNs (to protect the active compound from metabolic reactions) and to assess the pharmaco-technological parameters of the nanoparticles. The analyses yielded promising results. The particle sizes were around 200 nm, and the tests did not reveal particular differences in size between SLNs and SLN-SA. The PDI was about 0.300 and remained constant over the 2 months. The encapsulation efficiency and the release study showed the optimal capacity of the nanoparticles to incorporate sinapic acid, with a release profile characterized by an initial burst effect (due to the free fraction of SA) followed by a long-lasting liberation from SLN. Calorimetric studies were conducted on empty MLVs of DMPC and MLVs of DMPC incorporating a molar fraction of SA equal to the percentage found in SLNs, as well as on empty SLNs and SLNs loaded with SA. The results showed that the effect of SA on MLVs was significant, particularly in terms of enthalpy reduction; the presence of a unique main transition peak hinted at a uniform distribution of SA inside the MLVs [39,40]; on the other hand, SLNs and SLN-SA demonstrated a similar calorimetric profile.

To assess the capacity of SLN-SA to permit the interaction of SA with the biomembrane model made of DMPC over time, the SLN-SA/MLV interaction was investigated, which thoroughly confirmed the ability of the carrier to permit said interaction. The MLV signal of the last scan of the calorimetric kinetics experiment was indeed similar to the thermal peak obtained following the direct incorporation of sinapic acid inside MLVs; however, the effect

of SLNs on the MLVs should be accounted for, explaining the thermotropic differences (Figure 7).

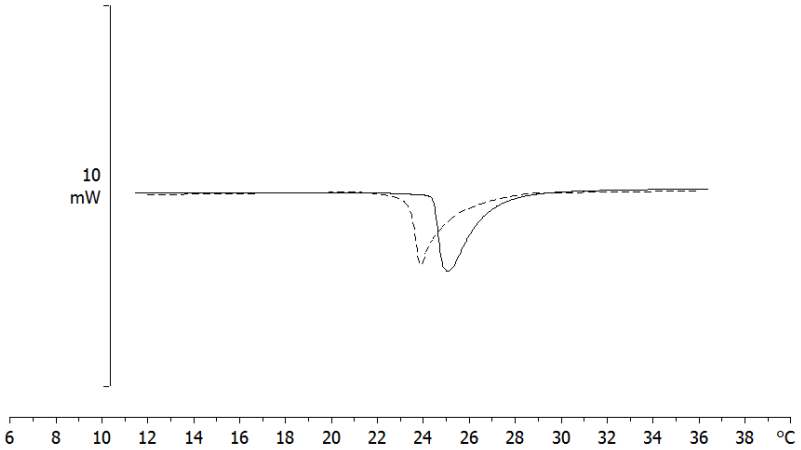

Figure 7. Calorimetric curves, in heating mode, of MLVs from the last scan of the calorimetric kinetics experiment (dotted line) and of MLVs obtained following the direct incorporation of sinapic acid (continuous line).

5. Conclusions

In conclusion, SLN-SA was found to be efficient as a potential carrier for the delivery of sinapic acid, possibly allowing its action while protecting it from metabolization and excretion processes. To further confirm these data, this nanoparticle-based formulation can be tested, in comparison to free sinapic acid, in future biological and biochemical experiments. Experiments should, firstly, be conducted in vitro to assess its capacity to reduce both mitochondrial and nonmitochondrial oxidative stress, as well as other problems related to inflammation and oxidative damage. Other studies have pointed out the importance of lipid base systems as carriers for other phenolic compounds, such as ferulic acid and caffeic acid [45,46]. The preparation of sinapic acid-loaded SLNs can enable the flexible use of this formulation in clinical settings. SLNs, depending on their dimensions, can be administered orally or parenterally. In addition, SLNs are suitable for cutaneous application, due to the affinity of their matrix to intercellular lipids in the stratum corneum.

Supplementary Materials: The following supporting information can be downloaded at: https://www.mdpi.com/article/10.3390/micro3020034/s1, Figure S1: SEM images of SLN and SLN-SA.

Author Contributions: Conceptualization, S.R., G.G. and M.G.S.; methodology, S.R. and G.G.; software, S.R. and G.G.; validation, S.R. and M.G.S.; formal analysis, S.R. and M.G.S.; investigation, S.R. and G.G.; resources, M.G.S.; data curation, S.R. and G.G.; writing—original draft preparation, S.R. and M.G.S.; writing—review and editing, S.R., G.G. and M.G.S.; visualization, S.R., G.G. and M.G.S.; supervision, M.G.S.; project administration, M.G.S. All authors have read and agreed to the published version of the manuscript.

Funding: This research received no external funding.

Institutional Review Board Statement: Not applicable.

Informed Consent Statement: Not applicable.

Data Availability Statement: Data were generated at the Department of Drug and Health Sciences, University of Catania. Data supporting the results of this study are available from the corresponding author on request.

Conflicts of Interest: The authors declare no conflict of interest.

References

1. Teixeira, J.; Gaspar, A.; Garrido, E.M.; Garrido, J.; Borges, F. Hydroxycinnamic Acid Antioxidants: An Electrochemical Overview. *BioMed Res. Int.* **2013**, *2013*, 251754. [CrossRef]
2. Kikuzaki, H.; Hisamoto, M.; Hirose, K.; Akiyama, K.; Taniguchi, H. Antioxidant Properties of Ferulic Acid and Its Related Compounds. *J. Agric. Food Chem.* **2002**, *50*, 2161–2168. [CrossRef]
3. Cos, P.; Rajan, P.; Vedernikova, I.; Calomme, M.; Pieters, L.; Vlietinck, A.J.; Augustyns, K.; Haemers, A.; Berghe, D.V. In Vitro Antioxidant Profile of Phenolic Acid Derivatives. *Free. Radic. Res.* **2002**, *36*, 711–716. [CrossRef] [PubMed]
4. Anticancer Activity of Sinapic Acid by Inducing Apoptosis in HT-29 Human Colon Cancer Cell Line. Available online: https://cdnsciencepub.com/doi/10.1139/cjpp-2022-0523 (accessed on 19 April 2023).
5. Rostami, A.; Baluchnejadmojarad, T.; Roghani, M. Sinapic Acid Ameliorates Paracetamol-Induced Acute Liver Injury through Targeting Oxidative Stress and Inflammation. *Mol. Biol. Rep.* **2022**, *49*, 4179–4191. [CrossRef]
6. Stanely Mainzen Prince, P.; Dey, P.; Roy, S.J. Sinapic Acid Safeguards Cardiac Mitochondria from Damage in Isoproterenol-Induced Myocardial Infarcted Rats. *J. Biochem. Mol. Toxicol.* **2020**, *34*, e22556. [CrossRef] [PubMed]
7. Tungalag, T.; Yang, D.K. Sinapic Acid Protects SH-SY5Y Human Neuroblastoma Cells against 6-Hydroxydopamine-Induced Neurotoxicity. *Biomedicines* **2021**, *9*, 295. [CrossRef] [PubMed]
8. Huang, T.; Zhao, D.; Lee, S.; Keum, G.; Yang, H.O. Sinapic Acid Attenuates the Neuroinflammatory Response by Targeting AKT and MAPK in LPS-Activated Microglial Models. *Biomol. Ther.* **2023**, *31*, 276–284. [CrossRef]
9. Yoon, B.H.; Jung, J.W.; Lee, J.-J.; Cho, Y.-W.; Jang, C.-G.; Jin, C.; Oh, T.H.; Ryu, J.H. Anxiolytic-like Effects of Sinapic Acid in Mice. *Life Sci.* **2007**, *81*, 234–240. [CrossRef]
10. Maddox, C.E.; Laur, L.M.; Tian, L. Antibacterial Activity of Phenolic Compounds against the Phytopathogen *Xylella fastidiosa*. *Curr. Microbiol.* **2010**, *60*, 53–58. [CrossRef]
11. Pandi, A.; Kalappan, V.M. Pharmacological and Therapeutic Applications of Sinapic Acid—An Updated Review. *Mol. Biol. Rep.* **2021**, *48*, 3733–3745. [CrossRef] [PubMed]
12. Shivashankara, K.S.; Acharya, S.N. Bioavailability of Dietary Polyphenols and the Cardiovascular Diseases. *TONUTRAJ* **2010**, *3*, 227–241. [CrossRef]
13. Piazzon, A.; Forte, M.; Nardini, M. Characterization of Phenolics Content and Antioxidant Activity of Different Beer Types. *J. Agric. Food Chem.* **2010**, *58*, 10677–10683. [CrossRef]
14. da Silveira, T.F.F.; Cajaíba, L.M.; Valentin, L.; Baréa, B.; Villeneuve, P.; Castro, I.A. Effect of Sinapic Acid Ester Derivatives on the Oxidative Stability of Omega-3 Fatty Acids Rich Oil-in-Water Emulsions. *Food Chem.* **2020**, *309*, 125586. [CrossRef] [PubMed]
15. Savjani, K.T.; Gajjar, A.K.; Savjani, J.K. Drug Solubility: Importance and Enhancement Techniques. *ISRN Pharm.* **2012**, *2012*, 195727. [CrossRef]
16. Wang, J.; Cao, Y.; Sun, B.; Wang, C. Characterisation of Inclusion Complex of Trans-Ferulic Acid and Hydroxypropyl-β-Cyclodextrin. *Food Chem.* **2011**, *124*, 1069–1075. [CrossRef]
17. Demurtas, M.; Onnis, V.; Zucca, P.; Rescigno, A.; Lachowicz, J.I.; De Villiers Engelbrecht, L.; Nieddu, M.; Ennas, G.; Scano, A.; Mocci, F.; et al. Cholinium-Based Ionic Liquids from Hydroxycinnamic Acids as New Promising Bioactive Agents: A Combined Experimental and Theoretical Investigation. *ACS Sustain. Chem. Eng.* **2021**, *9*, 2975–2986. [CrossRef]
18. Sinha, A.S.; Khandavilli, U.B.R.; O'Connor, E.L.; Deadman, B.J.; Maguire, A.R.; Lawrence, S.E. Novel Co-Crystals of the Nutraceutical Sinapic Acid. *CrystEngComm* **2015**, *17*, 4832–4841. [CrossRef]
19. Ahad, A.; Bin Jardan, Y.A.; Raish, M.; Al-Mohizea, A.M.; Al-Jenoobi, F.I. Hydroxypropyl-β-Cyclodextrin for Delivery of Sinapic Acid via Inclusion Complex Prepared by Solvent Evaporation Method. *Processes* **2022**, *10*, 2046. [CrossRef]
20. Kishida, K.; Matsumoto, H. Urinary Excretion Rate and Bioavailability of Chlorogenic Acid, Caffeic Acid, p-Coumaric Acid, and Ferulic Acid in Non-Fasted Rats Maintained under Physiological Conditions. *Heliyon* **2019**, *5*, e02708. [CrossRef] [PubMed]
21. Castelli, F.; Puglia, C.; Sarpietro, M.G.; Rizza, L.; Bonina, F. Characterization of Indomethacin-Loaded Lipid Nanoparticles by Differential Scanning Calorimetry. *Int. J. Pharm.* **2005**, *304*, 231–238. [CrossRef] [PubMed]
22. Lingayat, V.J.; Zarekar, N.S.; Shendge, R.S. Solid Lipid Nanoparticles: A Review. *Nanosci. Nanotechnol. Res.* **2017**, *4*, 67–72.
23. Mukherjee, S.; Ray, S.; Thakur, R.S. Solid Lipid Nanoparticles: A Modern Formulation Approach in Drug Delivery System. *Ind. J. Pharm. Sci.* **2009**, *71*, 349–358. [CrossRef]
24. Müller, R.H.; Radtke, M.; Wissing, S.A. Solid Lipid Nanoparticles (SLN) and Nanostructured Lipid Carriers (NLC) in Cosmetic and Dermatological Preparations. *Adv. Drug Deliv. Rev.* **2002**, *54*, S131–S155. [CrossRef]
25. Russo, S.; Torrisi, C.; Cardullo, N.; Muccilli, V.; Mantia, A.L.; Castelli, F.; Acquaviva, R.; Sarpietro, M.G. Ethyl Protocatechuate Encapsulation in Solid Lipid Nanoparticles: Assessment of Pharmacotechnical Parameters and Preliminary In Vitro Evaluation for Colorectal Cancer Treatment. *Pharmaceutics* **2023**, *15*, 394. [CrossRef] [PubMed]
26. Torrisi, C.; Cardullo, N.; Muccilli, V.; Tringali, C.; Castelli, F.; Sarpietro, M.G. Characterization and Interaction with Biomembrane Model of Benzo[k,l]Xanthene Lignan Loaded Solid Lipid Nanoparticles. *Membranes* **2022**, *12*, 615. [CrossRef] [PubMed]
27. Gaspar, D.P.; Faria, V.; Gonçalves, L.M.D.; Taboada, P.; Remuñán-López, C.; Almeida, A.J. Rifabutin-Loaded Solid Lipid Nanoparticles for Inhaled Antitubercular Therapy: Physicochemical and in Vitro Studies. *Int. J. Pharm.* **2016**, *497*, 199–209. [CrossRef] [PubMed]
28. Wang, J.-X.; Sun, X.; Zhang, Z.-R. Enhanced Brain Targeting by Synthesis of 3′,5′-Dioctanoyl-5-Fluoro-2′-Deoxyuridine and Incorporation into Solid Lipid Nanoparticles. *Eur. J. Pharm. Biopharm.* **2002**, *54*, 285–290. [CrossRef] [PubMed]

29. Venkateswarlu, V.; Manjunath, K. Preparation, Characterization and in Vitro Release Kinetics of Clozapine Solid Lipid Nanoparticles. *J. Control. Release* **2004**, *95*, 627–638. [CrossRef]
30. Greening, D.W.; Simpson, R.J. A Centrifugal Ultrafiltration Strategy for Isolating the Low-Molecular Weight (<or=25K) Component of Human Plasma Proteome. *J. Proteom.* **2010**, *73*, 637–648. [CrossRef]
31. Brito Raj, S.; Chandrasekhar, K.B.; Reddy, K.B. Formulation, in-Vitro and in-Vivo Pharmacokinetic Evaluation of Simvastatin Nanostructured Lipid Carrier Loaded Transdermal Drug Delivery System. *Future J. Pharm. Sci.* **2019**, *5*, 9. [CrossRef]
32. Yadav, S.; Gupta, S. Development and in Vitro Characterization of Docetaxel-Loaded Ligand Appended Solid Fat Nanoemulsions for Potential Use in Breast Cancer Therapy. *Artif. Cells Nanomed. Biotechnol.* **2015**, *43*, 93–102. [CrossRef] [PubMed]
33. Torrisi, C.; Cardullo, N.; Russo, S.; La Mantia, A.; Acquaviva, R.; Muccilli, V.; Castelli, F.; Sarpietro, M.G. Benzo[k,l]Xanthene Lignan-Loaded Solid Lipid Nanoparticles for Topical Application: A Preliminary Study. *Molecules* **2022**, *27*, 5887. [CrossRef] [PubMed]
34. Walde, P. Preparation of Vesicles (Liposomes). In *Encyclopedia of Nanoscience and Nanotechnology*; Nalwa, H.S., Ed.; American Scientific Publishers: Los Angeles, CA, USA, 2004; Volume 9.
35. Ladbrooke, B.D.; Chapman, D. Thermal Analysis of Lipids, Proteins and Biological Membranes. A Review and Summary of Some Recent Studies. *Chem. Phys. Lipids* **1969**, *3*, 304–356. [CrossRef] [PubMed]
36. Cevc, G. Polymorphism of the Bilayer Membranes in the Ordered Phase and the Molecular Origin of the Lipid Pretransition and Rippled Lamellae. *Biochim. Biophys. Acta* **1991**, *1062*, 59–69. [CrossRef]
37. Gardikis, K.; Hatziantoniou, S.; Viras, K.; Wagner, M.; Demetzos, C. A DSC and Raman Spectroscopy Study on the Effect of PAMAM Dendrimer on DPPC Model Lipid Membranes. *Int. J. Pharm.* **2006**, *318*, 118–123. [CrossRef]
38. Basso, L.G.M.; Rodrigues, R.Z.; Naal, R.M.Z.G.; Costa-Filho, A.J. Effects of the Antimalarial Drug Primaquine on the Dynamic Structure of Lipid Model Membranes. *Biochim. Biophys. Acta BBA—Biomembr.* **2011**, *1808*, 55–64. [CrossRef]
39. Lambros, M.P.; Rahman, Y.E. Effects of Cyclosporin A on Model Lipid Membranes. *Chem. Phys. Lipids* **2004**, *131*, 63–69. [CrossRef]
40. Alves, I.D.; Goasdoué, N.; Correia, I.; Aubry, S.; Galanth, C.; Sagan, S.; Lavielle, S.; Chassaing, G. Membrane Interaction and Perturbation Mechanisms Induced by Two Cationic Cell Penetrating Peptides with Distinct Charge Distribution. *Biochim. Biophys. Acta* **2008**, *1780*, 948–959. [CrossRef] [PubMed]
41. Interaction of Dopamine with Zwitterionic DMPC and Anionic DMPS Multilamellar Vesicle Membranes | Langmuir. Available online: https://pubs.acs.org/doi/full/10.1021/acs.langmuir.1c02184 (accessed on 21 March 2023).
42. Ezer, N.; Sahin, I.; Kazanci, N. Alliin Interacts with DMPC Model Membranes to Modify the Membrane Dynamics: FTIR and DSC Studies. *Vib. Spectrosc.* **2017**, *89*, 1–8. [CrossRef]
43. Cherng, Y.-G.; Tsai, C.-C.; Chung, H.-H.; Lai, Y.-W.; Kuo, S.-C.; Cheng, J.-T. Antihyperglycemic Action of Sinapic Acid in Diabetic Rats. *J. Agric. Food Chem.* **2013**, *61*, 12053–12059. [CrossRef]
44. Yang, C.; Deng, Q.; Xu, J.; Wang, X.; Hu, C.; Tang, H.; Huang, F. Sinapic Acid and Resveratrol Alleviate Oxidative Stress with Modulation of Gut Microbiota in High-Fat Diet-Fed Rats. *Food Res. Int.* **2019**, *116*, 1202–1211. [CrossRef] [PubMed]
45. Trombino, S.; Cassano, R.; Ferrarelli, T.; Barone, E.; Picci, N.; Mancuso, C. Trans-Ferulic Acid-Based Solid Lipid Nanoparticles and Their Antioxidant Effect in Rat Brain Microsomes. *Colloids Surf. B Biointerfaces* **2013**, *109*, 273–279. [CrossRef] [PubMed]
46. Hallan, S.S.; Sguizzato, M.; Drechsler, M.; Mariani, P.; Montesi, L.; Cortesi, R.; Björklund, S.; Ruzgas, T.; Esposito, E. The Potential of Caffeic Acid Lipid Nanoparticulate Systems for Skin Application: In Vitro Assays to Assess Delivery and Antioxidant Effect. *Nanomaterials* **2021**, *11*, 171. [CrossRef] [PubMed]